Adsorption enhanced rapid catalytic degradation of ofloxacin by CoS₂@montmorillonite catalyst via peroxymonosulfate activation

Peiping Hong,[a] Lian Wu,[a, b] Yifang Zhao,[a] Yue Yu,[a] Shuxi Gao,[a] Bing Liao,*[a] and Hao Pang*[a]

a. *Institute of Chemical Engineering, Guangdong Academy of Sciences, Guangzhou, Guangdong 510665 (P. R. China).*

b. *Guangxi Key Laboratory of Petrochemical Resource Processing and Process Intensification Technology, Guangxi University, Nanning 530004, (P. R. China)*

* *Corresponding authors. E-mail address: liaobing@gic.ac.cn; panghao@gdcri.com.*

Experimental

1 Preparation of CoS$_2$@MMT catalysts

CoS$_2$@MMT were prepared according to our previous research without any pre-treatment[29]. Typically, 1g MMT was added into 70 mL CoCl$_2$·6H$_2$O solution and vigorously stirred for 2 h at 60 °C to realize the cobalt cation exchange. Then, Na$_2$S$_2$O$_3$·5H$_2$O (two equivalent to CoCl$_2$·6H$_2$O) was added to the above suspension, transferred to a Teflon autoclave and reacted at 150 °C for 15 h. Finally, the obtained CoS$_2$@MMT were washed with ethyl alcohol/water, and vacuum dried at 60 °C. Specifically, the addition of CoCl$_2$·6H$_2$O were 5, 10 and 20 mmol and the corresponding samples were noted as 5CoS$_2$@MMT, 10CoS$_2$@MMT and 20CoS$_2$@MMT, respectively.

2 Materials characterization

Powder X-ray diffraction (PXRD) were tested on a Rigaku SmartLab 9 kW with Cu Kα radiation. Scanning electron microscopy (SEM) figures and the related elemental mapping were recorded in TESCAN MIRA LMS. Transmission electron microscopy (TEM) images were tested on TF20. Micromeritics ASAP 2460 system was applied to test the nitrogen gas adsorption-desorption isotherms at 77 K after activated at 150 °C for 12 h. X-ray photoelectron spectroscopy (XPS) were carried out on Thermo Scientific K-Alpha system with an Al Kαsource (1486.6 eV). Thermogravimetric analysis (TGA) was tested on RIGAKU TG-DTA8122 under an air atmosphere with a heating rate of 10 °C min^{-1} in the range of 80-700 °C. Electron paramagnetic resonance (EPR) was rested on Bruker EMXplus-6/1. Ultra-performance liquid chromatography-mass spectrometry (UPLC-MS) was conducted on a Waters Acquity UPLC system coupled with a Waters Xevo-G2 QTOF mass spectrometer. The mobile phases consist of (A) 0.1% formic acid-water and (B) MeOH and the flow rate is set at 0.3 mL/min.

3 Adsorption experiments

The adsorption capacity was studied by adding the composite (100 mg/L) in 100 mL OFL solution (20 ppm) and shaken at room temperature. At certain time interval, 2 mL mixture was removed and filtered by 45 μm PTFE membrane. The residual contents of OFL were confirmed by the peak intensity at 288 nm by UV-vis spectrophotometer.

4 Catalytic degradation experiments

The catalytic activity of the composites was evaluated by the catalytic degradation of OFL via the PSM activation at room temperature and repeated for three times. Typically, 5 mg of catalysts were added in 50 mL OFL solution in 100 mL glass beaker. After sonicated and shocked for 30 min to reach the adsorption-desorption equilibrium, PMS stock solution (0.5 mL, 1 mM) was added to initiate the AOP reaction. During catalytic reaction, 1 mL aliquots of the suspension were obtained at certain time intervals, filtered by a 0.45 μm PTFE membrane and mixed with 1 mL methanol rapidly deplete the residual active species. The concentration of OFL was determined by UV-vis spectrophotometer, through monitoring the peak intensity at 288 nm. The removal rate (%) was determined by the following formula:

$$Removal\,rate\,(\%) = \frac{C_0 - C_t}{C_0} * 100$$

(1)

The OFL removal process was analysed with the pseudo-second-order kinetics. C_0 and C_t are the concentrations of OFL at 0 min and t min, respectively. K value is pseudo-second-order constant (min^{-1}) analysed by the following formula,

$$\frac{1}{C_t} - \frac{1}{C_0} = K \cdot t$$

(2)

The relayed fitting results were listed in Table S2 and S3.

The recycling experiments were conducted by adding the OFL and PMS stock solution in sequence to start a new degradation with the same catalysts.
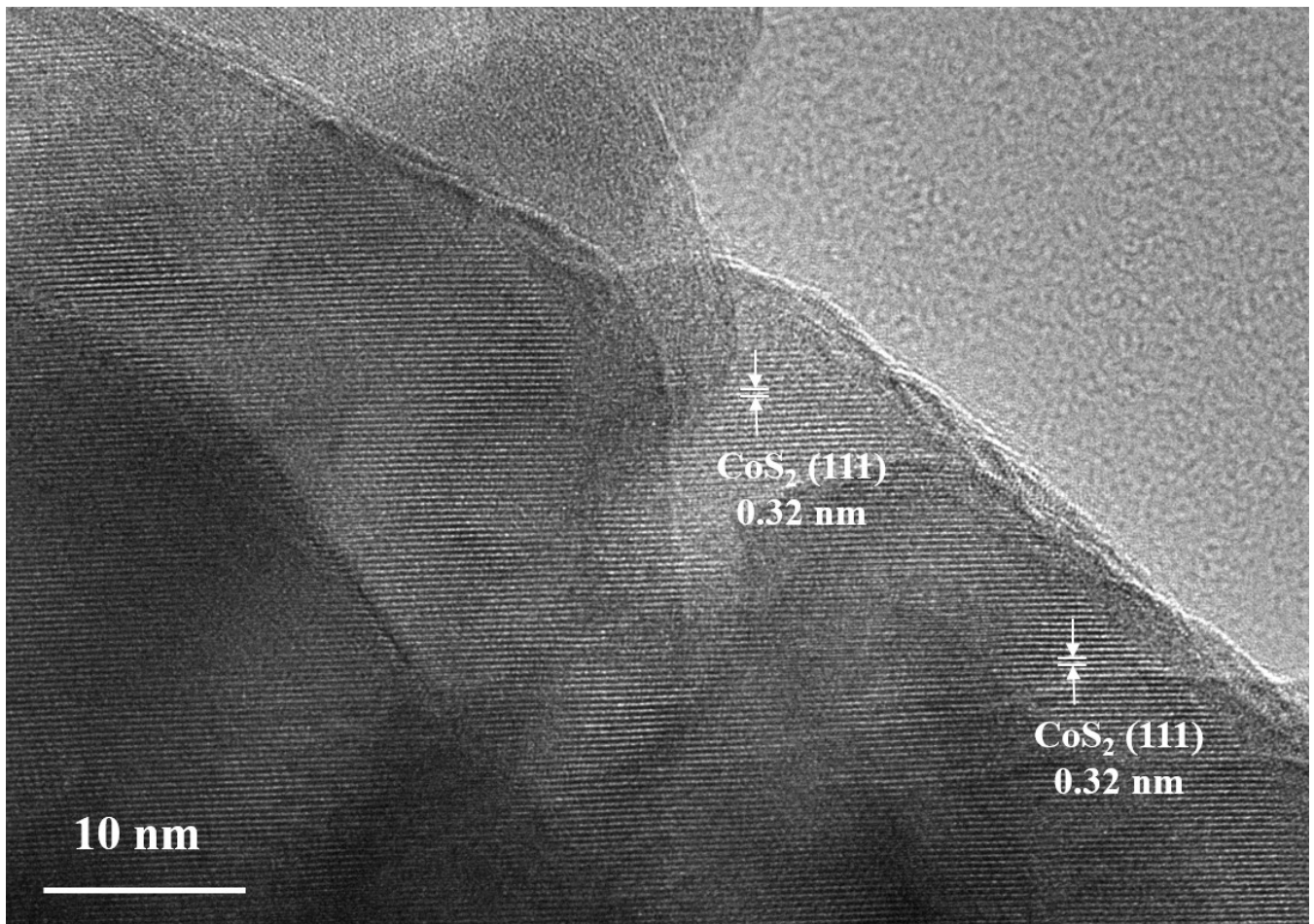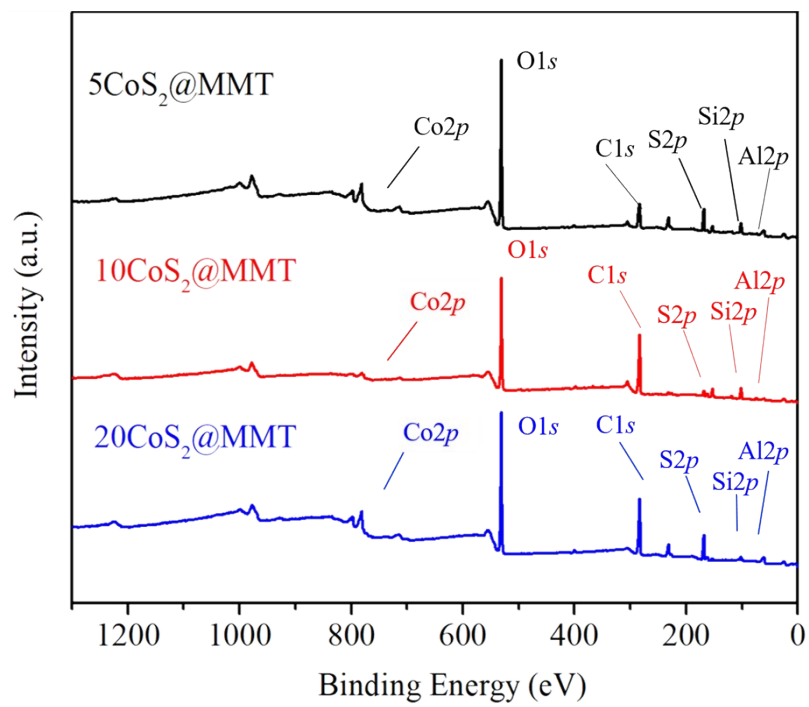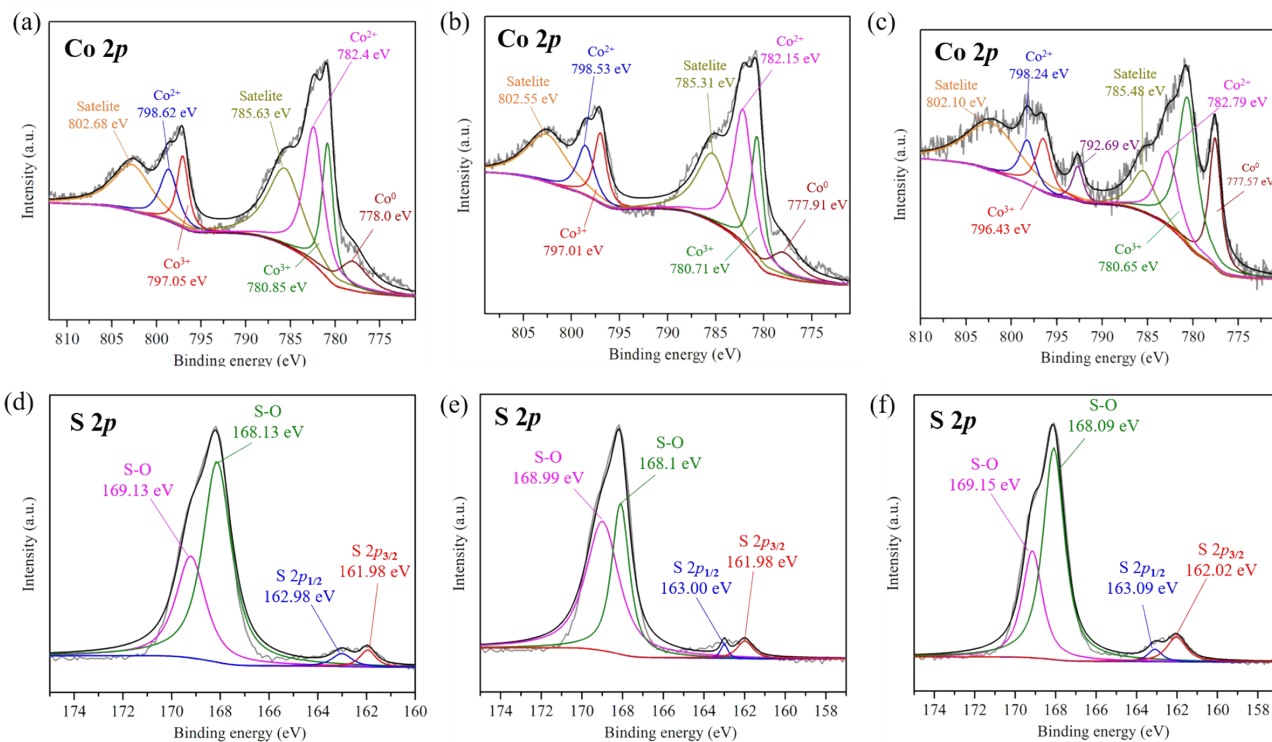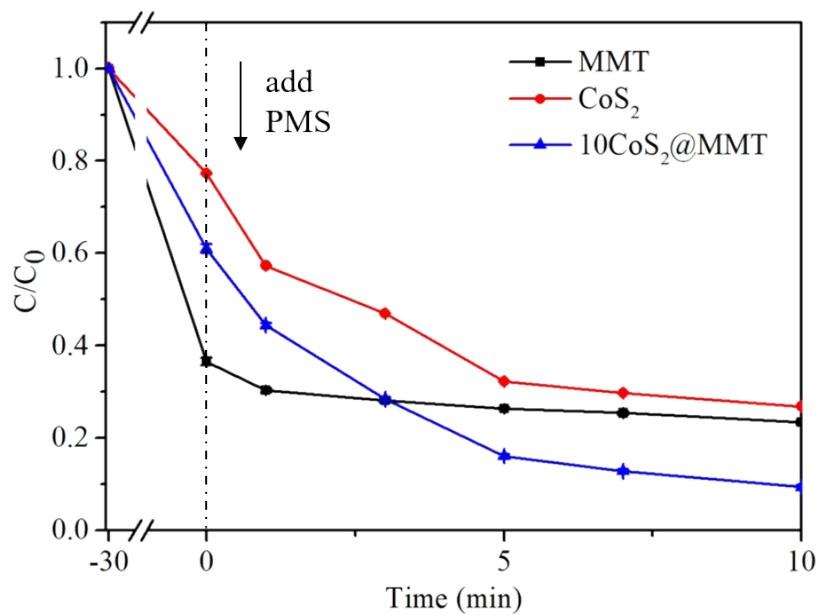
Figure S1. TEM images of 10CoS$_2$@MMT.

Figure S2. XPS survey spectra of 5CoS$_2$@MMT, 10CoS$_2$@MMT and 20CoS$_2$@MMT.

Figure S3. High-resolution scans of Co $2p$ and S $2p$ of the XPS survey spectra of 5CoS$_2$@MMT (a, d), 10CoS$_2$@MMT (b, e) and 20CoS$_2$@MMT (c, f), respectively.

Figure S4. The OFL degradation of MMT, CoS$_2$ and CoS$_2$@MMT without shock operation.
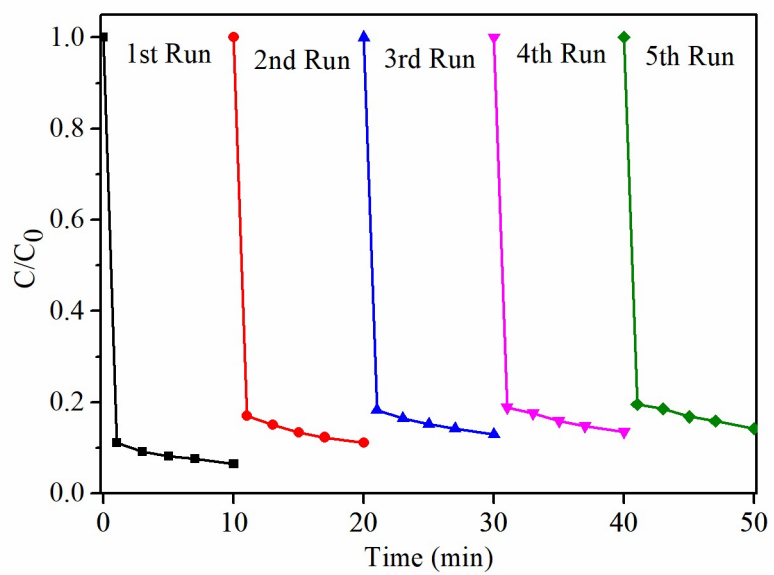
Figure S5. Reusability of 10CoS$_2$@MMT as AOP catalyst to degrade OFL.
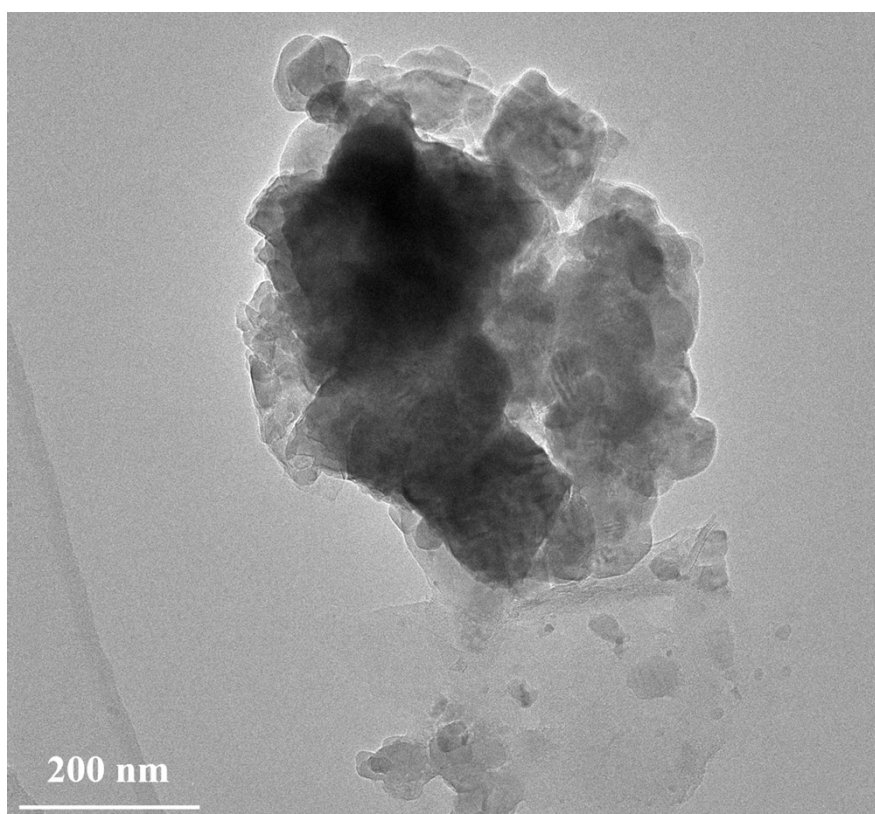
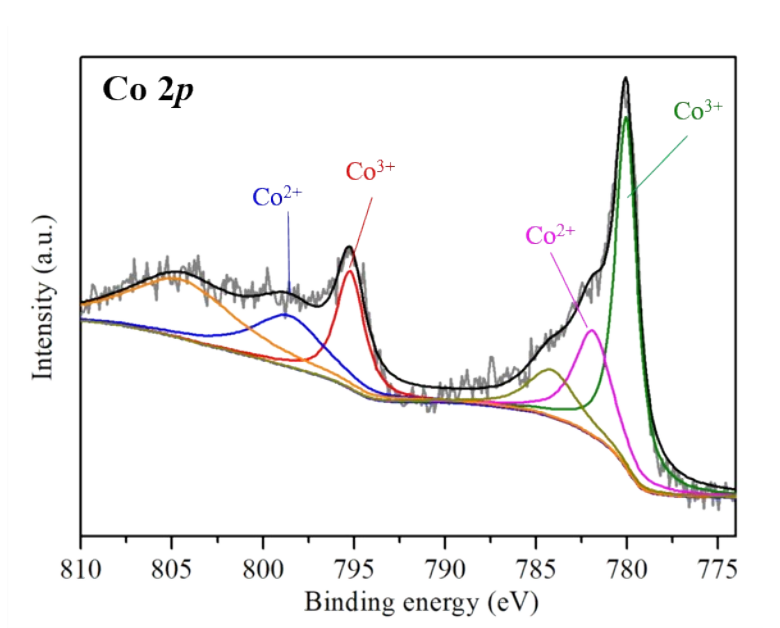**Figure S6.** TEM image of the reused 10CoS$_2$@MMT.

Figure S7. High-resolution scans of Co 2*p* of the XPS survey spectra of 10CoS$_2$@MMT after degradation experiments.
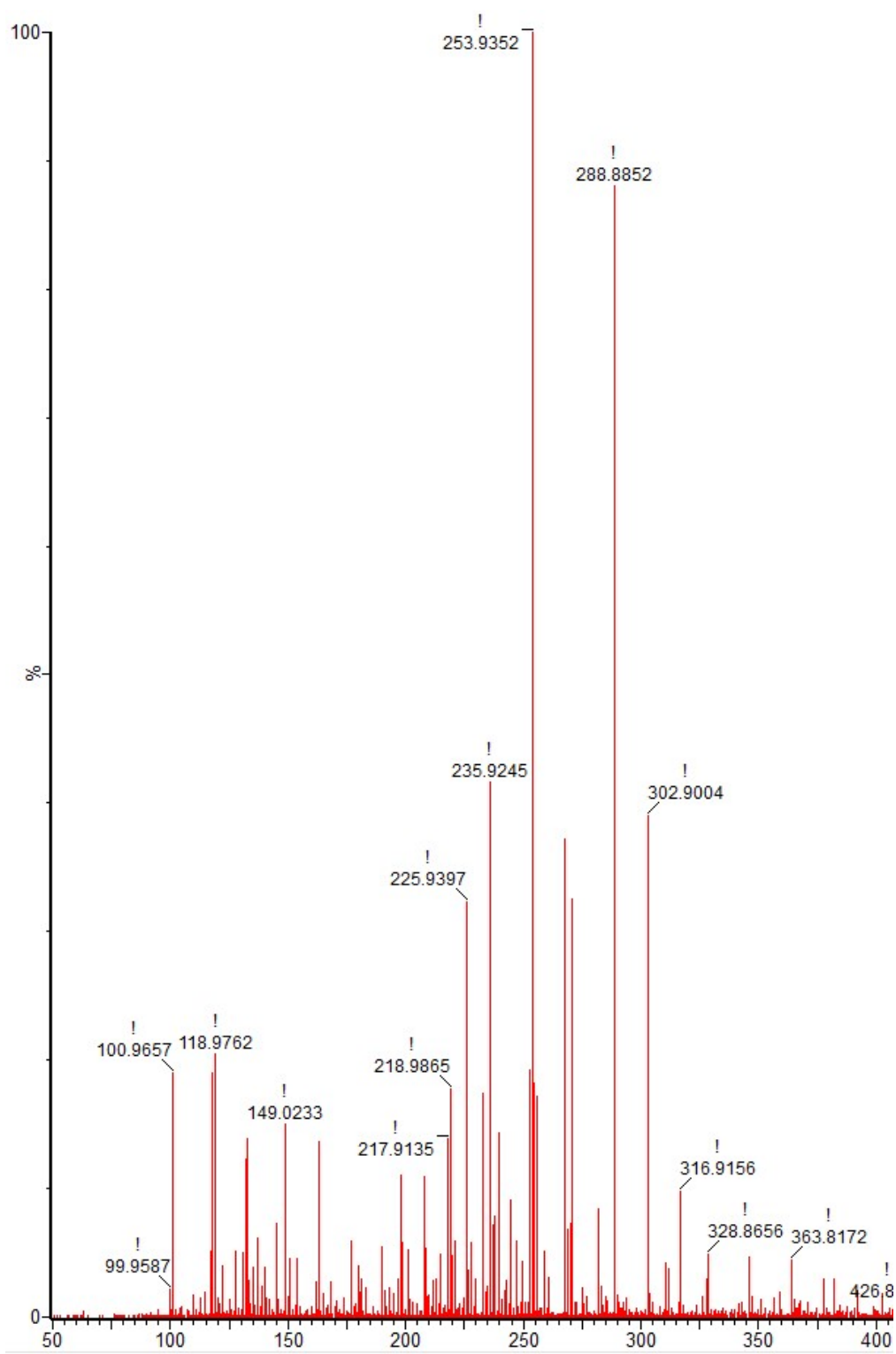
Figure S8. MS spectrum of the products in 10CoS$_2$@MMT system.

Table S1. Porosities of MMT, 5CoS$_2$@MMT, 10CoS$_2$@MMTand 20CoS$_2$@MMT

Sample	S$_{BET}$ (m$^2\cdot$g^{-1})	Average pore diameter (nm)	Pore volume (cm$^3\cdot$g^{-1})
MMT	50.10	7.33	0.11
5CoS$_2$@MMT	12.79	8.59	0.04
10CoS$_2$@MMT	11.04	11.08	0.03
20CoS$_2$@MMT	7.33	12.14	0.03

Table S2 Catalytic performance of 10CoS$_2$@MMT in OFL degradation under different conditions.

Catalyst	OFL Concentration (ppm)	Catalysts dosage (mg/L)	PMS dosage (mM)	Initial pH value	Total removal efficiency (%)	K (min^{-1})	R^2
10CoS$_2$@MMT	10	100	0.66	No adjusted	97.6	0.287	0.997
10CoS$_2$@MMT	20	100	0.66	No adjusted	96.7	0.111	0.990
10CoS$_2$@MMT	30	100	0.66	No adjusted	94.6	0.044	0.989
10CoS$_2$@MMT	40	100	0.66	No adjusted	93.0	0.027	0.990
10CoS$_2$@MMT	50	100	0.66	No adjusted	91.4	0.018	0.991
10CoS$_2$@MMT	20	40	0.66	No adjusted	94.4	0.066	0.971
10CoS$_2$@MMT	20	200	0.66	No adjusted	96.4	0.114	0.990
10CoS$_2$@MMT	20	400	0.66	No adjusted	97.5	0.131	0.996
10CoS$_2$@MMT	20	100	0.33	No adjusted	95.6	0.075	0.961
10CoS$_2$@MMT	20	100	0.99	No adjusted	96.1	0.146	0.982
10CoS$_2$@MMT	20	100	1.32	No adjusted	97.6	0.183	0.990
10CoS$_2$@MMT	20	100	0.66	3	95.5	0.089	0.987
10CoS$_2$@MMT	20	100	0.66	5	93.0	0.065	0.927
10CoS$_2$@MMT	20	100	0.66	7	97.3	0.103	0.994
10CoS$_2$@MMT	20	100	0.66	9	97.2	0.114	0.985

Table S3 Catalytic performance of 10CoS$_2$@MMT in OFL degradation with various interferences.

Interfences	OFL Concentration (ppm)	Catalysts dosage (mg/L)	PMS dosage (mM)	Initial pH value	Total removal efficiency (%)	K (min^{-1})	R^2
40 ppm Na$_2$SO$_4$	20	100	0.66	No adjusted	95.2	0.0883	0.992
200 ppm Na$_2$SO$_4$	20	100	0.66	No adjusted	92.1	0.0682	0.989
40 ppm NaNO$_3$	20	100	0.66	No adjusted	95.1	0.0859	0.989
200 ppm NaNO$_3$	20	100	0.66	No adjusted	93.2	0.0481	0.991
40 ppm NaHCO$_3$	20	100	0.66	No adjusted	97.7	0.121	0.972
200 ppm NaHCO$_3$	20	100	0.66	No adjusted	77.6	0.0067	0.987
40 ppm NaCl	20	100	0.66	No adjusted	81.3	0.0173	0.991
200 ppm NaCl	20	100	0.66	No adjusted	79.8	0.0130	0.990
0.2 mM Methanol	20	100	0.66	No adjusted	77.6	0.0084	0.992
0.2 mM TBA	20	100	0.66	No adjusted	87.0	0.0109	0.976
1 mM p-BQ	20	100	0.66	No adjusted	84.2	0.0204	0.992
1.5 mM FFA	20	100	0.66	No adjusted	36	-	-

Table S4 Predicted ecotoxicity of OFL and its degradation intermediates.

Compound	Acute toxicity (mg/L) or (mg/kg)		Development toxicity	Mutagenicity	Bioaccumulation factor
	Fathead minnow LC50 (96 h)	Daphnia magna LC50 (48 h)			
OFL	0.8	16.78	1.03	0.65	4.26
P1	0.49	13.32	0.90	0.64	4.39
P2	123.81	223.05	0.60	0.44	0.43
P3	5.35	6.37	0.53	0.86	**70.43**
P4	380.57	61.23	0.63	0.28	3.64
P5	1305.91	170.98	0.51	0.24	1.34
P6	209.04	91.60	0.37	0.27	3.59
P7	1.80	9.57	1.02	0.67	**25.15**
P8	2.44	7.40	0.83	0.65	**14.54**
P9	4.18	4.41	0.80	0.71	**30.99**
P10	170.46	112.20	0.88	0.35	**22.01**
P11	100.60	45.61	0.45	0.20	0.73
P12	65.77	39.25	0.57	0.10	0.60
P13	0.82	21.98	0.98	0.58	4.33
P14	0.51	4.39	0.68	0.39	3.28
P15	2.96	6.13	1.03	0.55	2.22
P16	4.44	2.59	0.76	0.94	**15.76**
P17	416.94	130.35	0.82	0.72	0.72
P18	1.57	28.61	1.05	0.61	**17.37**
P19	4.09	10.14	0.82	0.64	**19.74**
P20	5.35	30.79	0.78	0.72	4.26

Note: ▮ Not harmful or negative; ▮ Toxic; ▮ Very toxic, harmful or positive

Intermediates	Chemical formula	Measured mass (m/z)	Structure
P1	C$_{18}$H$_{22}$FN$_3$O$_5$	378.81	
P2	C$_4$H$_4$O$_4$	118.98	
P3	C$_{14}$H$_{20}$FN$_3$O	264.85	
P4	C$_7$H$_{15}$FN$_2$	149.02	
P5	C$_5$H$_{12}$N$_2$	100.97	
P6	C$_5$H$_{12}$N$_2$O$_2$	132.95	
P7	C$_{17}$H$_{20}$FN$_3$O$_2$	316.92	
P8	C$_{16}$H$_{18}$FN$_3$O$_2$	302.9	
P9	C$_{12}$H$_9$FNO$_2$	218.99	
P10	C$_{10}$H$_8$FNO$_4$	225.94	
P11	C$_9$H$_{10}$FNO$_3$	201.54	
P12	C$_9$H$_8$FNO$_2$	181.91	
P13	C$_{17}$H$_{18}$FN$_3$O$_4$	347.62	
P14	C$_{14}$H$_{13}$FN$_4$O$_6$	328.87	
P15	C$_{13}$H$_{11}$FN$_2$O$_4$	280.54	
P16	C$_{11}$H$_{14}$NO$_4$	225.94	
P17	C$_{12}$H$_{11}$FN$_2$O$_2$	235.92	
P18	C$_{16}$H$_{16}$FN$_3$O$_4$	328.87	

P19	$C_{15}H_{16}FN_3O_2$	288.89	$\overset{O}{\underset{\parallel}{}}$
P20	$C_{15}H_{17}N_3O_2$	270.63	$\overset{O}{\underset{\parallel}{}}$

Table S6. Performance comparison of CoS_2@MMT catalysts with other reported metal-based catalysts through PMS activation.

Type of catalyst	Reaction system	Reaction conditions	Performance	References
Calcined electroplating sludge	PMS	[OFL]=0.04 mM, [cat]=0.15 g/L, [PMS]=2.5 mM,	60 min 90%, K= 0.334 min⁻¹	[1]
$CuFe_2O_4$-Mt	PMS	[OFL]=40 ppm, [cat]=0.4 g/L, [PMS]=2.0 mM,	60 min 85.2%,	[2]
Co-CN	PMS	[tetracycline]=20ppm, [cat]=0.1 g/L, [PMS]=0.75 µM	30 min 93.3%	[3]
CoZn-CN	PMS	[tetracycline]=20ppm, [cat]=20 mg/L, [PMS]=0.2 g/L	30 min 99.8%, K= 1.344 min⁻¹	[4]
Fe_3C@BN-CNT	PMS	[doxycycline hydrochloride]=50 mg/L, [cat]=0.4 g/L, [PMS]=0.4 g/L	120 min 91.9%,	[5]
BC@FexC	peroxydisulfate (PDS)	[norfloxacin]=20 mg/L, [cat]=0.15 g/L, [PDS]=0.2 g/L	15 min 91.2%, K= 0.1043 min⁻¹	[6]
$CuFe_2O_4$@NC	PMS	[levofloxacin]=15 mg/L, [cat]=0.3 g/L, [PMS]= 0.3 g/L	90 min 84.87%,	[7]
CuCo@C	PMS	[ciprofloxacin]=10 mg/L, [cat]=0.25 g/L, [PMS]=0.25 g/L	30 min 90%,	[8]
$10CoS_2$@MMT	PMS	[OFL]=20 ppm, [cat]=100 mg/L, [PMS]=0.66 mM	10 min 96.7%, K= 0.111 min⁻¹	This work

References

[1]   G. Peng, C. Qi*, X. Wang, L. Zhou, Q. He*, W. Zhou, L. Chen. *Chemosphere*, 2021, 266, 128944.

[2]   X. –Q. Cao, F. Xiao, Z. –W. Lyu, X. –Y. Xie, Z. –X. Zhang, X. Dong, J. –X. Wang, X. –J. Lyu, Y. –Z. Zhang*, Y. Liang. *J. Water Process Eng.*, 2021, 44, 102359.

[3]   Q. Li, J. Liu, Z. Ren, Z. Wang, F. Mao, H. Wu*, R. Zhou, Y. Bu*. Chem. Eng. J., 2022, 429, 132269.

[4]   B. Hua, L. Zheng, A. Adeboye, F. Li*. Chem. Eng. J., 2022, 443, 136439.

[5]   S. Liang, H. –Y. Niu, H. Guo, C. –G. Niu*, C. Liang, J. –S. Li, N. Tang, L. –S. Lin, C. –W. Zheng. Chem. Eng. J., 2021, 405, 126686.

[6]   J. Tong, L. Chen, J. Cao, Z. Yang*, W. Xiong*, M. Jia, Y. Xiang, H. Peng. Sep. Purif. Technol., 2022, 294, 121064.

[7]   Z. –T. Dong, C. –G. Niu*, H. Guo, H. –Y. Niu, S. Liang, C. Liang, H. –Y. Liu, Y. –Y. Yang. Chem. Eng. J., 2021, 426, 130850.

[8]   M. –M. Chen, H. –Y. Niu, C. –G. Niu*, H. Guo, S. L., Y. –Y. Yang. J. Hazard. Mater., 2022, 424, 127196.